Seismic Assessment of Lightly Reinforced Buildings: A Study of Shear Demand vs. Supply

S.G. Chasioti
University of Stuttgart, Germany

S.J. Pantazopoulou
University of Cyprus, Cyprus / Democritus University of Thrace, Greece

D.V. Syntzirma
Municipality of Komotini Public Works Dept., Greece

15 WCEE
LISBOA 2012

SUMMARY:
Seismic assessment of reinforced concrete structures as prescribed by leading design code standards such as the EC8-III and FEMA 356 / ASCE/SEI-41 guidelines comprise a complex system of evaluation, but the various steps of this process are not vested with a uniform level of confidence as compared with the experimental results. Strength values can be estimated with sufficient accuracy only when the modes of failure are ductile. The level of accuracy degrades when considering brittle mechanisms of resistance, particularly when focusing on shear transfer and the associated deformation capacity. Today, after several years of persistent research including a vast number of experiments on columns under cyclic shear/moment/axial load combinations, the scatter of our analytical estimates as compared with the experimental shear strength values and observed modes of failure is unsettling, particularly when dealing with structural reinforced concrete members representative of old, substandard construction. In this paper, the problem of seismic shear is explored from first principles, with combined insight from experimental observation whenever assumptions need to be made. The procedures developed to assess shear strength of seismically loaded members are compared against measured experimental performances of a pertinent database of large scale columns with substandard details, tested under lateral load reversals that simulated earthquake effects.

Keywords: angle of compression struts, shear, contribution of concrete, modified compression field theory

1. INTRODUCTION

The procedure of estimating the strength, the deformation capacity and the expected mode of failure in primary members of a structure, that is, the complete process of seismic assessment of reinforced concrete structures, has been recently supported by background documents in both Europe and U.S. (EC8-III, FEMA 356 / ASCE/SEI-41, and most recently by the draft of the New Model Code by the *fib*). The acceptance criteria proposed, provide a complex system of evaluation, but the various steps of this process are not vested with a uniform level of confidence as compared with the experimental results. Strength values can be estimated with sufficient accuracy only if the involved modes of failure are ductile. The level of accuracy degrades when considering brittle mechanisms of resistance, and the associated deformation capacities, which are used as a basis for comparison with deformation demands. Yet, in the process of assessment it is critical to determine whether flexural yielding will precede shear failure (so as to ensure ductility) or whether a brittle failure ought to be anticipated. Even when flexural yielding may be supported it is also important to dependably estimate the ductility level beyond which shear strength may be assumed to have degraded below the flexural strength leading to a secondary post-yielding failure that limits the available deformation capacity [Pantazopoulou and Syntzirna 2010].

Traditionally, post-cracking shear strength had been estimated from summation of various separate resistances, attributed to concrete, to web reinforcement, to axial load, to aggregate interlock and to dowel action. It is a point of contention as to whether these mechanisms can actually be separated and independently estimated; it is more honest to admit that these may be viewed as successive refinements to the underlying basic truss model that was inspired by Mörsch more than 100 years ago, so as to improve its correlation with the test data.

After repeated efforts to identify the source of scatter between the existing models of seismic shear strength and the experimental measurements, it appears that the least understood variables are the following:

(1) The inclination of the major sliding plane (i.e. the angle θ forming between the primary diagonal crack heralding tension failure, with the longitudinal axis of the member), as this determines the number of stirrup layers mobilized in shear

(2) The participation of axial load in resisting shear

(3) The role of the aspect ratio of the member on shear strength (i.e., identifying and quantifying the shear – moment interaction envelope).

(4) The effective area of the concrete section mobilized in the "concrete" shear contribution.

Additional issues such as the influence of bond conditions, yield-penetration over the member away from the critical section, availability of confinement, slenderness ratio of longitudinal bars (referring to the unsupported length between successive stirrups) are also relevant, however they are not considered responsible for the dramatic discrepancies between calculations and test results – for this reason, they are considered beyond the scope of the present treatise.

Development of the model requires reference to experimental evidence. For that purpose two subsets of data are used: the first subset, comprising four large scale columns with substandard details tested under simulated seismic load by Woods and Matamoros (2009) are used to illustrate some the issues listed above and to highlight their implications in the analytical model. The second set of data is used to test the analytical model and is used as a benchmark for evaluation of concepts considered in the assessment procedures. This set of data comprises nineteen column tests carefully selected from the literature and conducted under combinations of compressive axial load – and a history of lateral displacement reversals of increasing magnitude.

A conceptual model for shear was derived whereby the plane of sliding failure, web reinforcement contribution and participation of concrete in resisting shear force was developed. The estimated shear strength magnitude is then used to prioritize the modes of failure and the associated deformation capacity (loss of load carrying capacity identified by a 20% drop in lateral load resistance after correction for P-Δ effects). The accuracy of the estimations of the various mechanisms of resistance that contribute to shear strength depends greatly on the inclination of the dominant plane of shear sliding, macroscopically associated with the principal diagonal tension crack that marks shear-related failure in reinforced concrete members. In this paper this is calculated as a function of the axial load and web longitudinal strain in accordance with basic concepts of concrete plane stress analysis.

2. EXPERIMENTAL DATABASE

Test specimens used in this paper in order to derive or to calibrate the shear model were presented in Woods and Matamoros 2010, Lam et al 2003, Sezen and Moehle 2004, Lynn et al 1996, Yavari et al 2009, Aboutaha et al 1996, Aboutaha et al 1999. The columns had details typical of pre–1970's construction tested either in double or single curvature, by imposed lateral load reversals. A constant axial load is applied to most of the columns, with the exception of the specimens by Aboutaha et al 1996 and 1999 (tests No 21 to 23 in Tab. 1), where tests were continued until complete loss of vertical load carrying capacity. Table 1 outlines specimen geometry, reinforcement and loading used in the tests. The cross section patterns are presented in Fig. 2; note that all the specimens considered have

90^0 hooks for anchorage of transverse reinforcement.

Most of the cases tested reportedly exhibited a dominant shear failure mechanism. The specimens by Woods and Matamoros 2010 and by Lam et al 2003 (tests No 1 to 4 in Tab. 1) failed in shear before the attainment of yielding, identified as condition 3 as per ASCE/SEI 41, whereas all other specimens are classified under condition 2 (shear failure after flexural yielding), with the exception of the specimens by Aboutaha et al 1996 and 1999 that failed due to insufficient development capacity of the lap splices in the critical region.Tests No 5 to 7 by Sezen and Moehle 2004, No 8 to 15 by Lynn et al. 1996 and No 16 to 20 by Yavari et al. 2009 are also included in the investigation.

Table 1. Test specimen materials and details (*a* is a cross section index with reference to Fig. 1)

Specimen ID; Serial No		angle	Geometry				l_s mm	$P/f_c{}'A_g$	$f_c{}'$ MPa	Long. Reinf.		Transverse Reinf.		
		θ	b mm	h mm	L_s/d	a				D_{bl} mm	f_{yl} MPa	d_t mm	f_{yh} MPa	s mm
Spec. 1[1]	1	35	457	457	3.75	1	–	0.32	33.0	8Ø28.7	445	9.5	372	457
Spec. 2[1]	2	35	457	457	3.75	1	–	0.21	33.0	8Ø28.7	445	9.5	372	457
Spec. 3[1]	3	36	457	457	3.75	1	–	0.62	17.0	8Ø32.3	445	9.5	372	457
X–9[2]	4	25	267	267	1.6	3	–	0.50	28.6	12Ø12+4Ø16	395	6.0	270	100
Spec. 1[3]	5	35	457	457	3.8	2	–	0.15	21.0	8Ø28.6	438	9.5	476	303
Spec. 2[3]	6	36	457	457	3.8	2	–	0.61	21.0	8Ø28.6	438	9.5	476	303
Spec. 4[3]	7	35	457	457	3.8	2	–	0.15	21.0	8Ø28.6	438	9.5	476	303
3CLH18[4]	8	35	457	457	3.87	1	–	0.09	25.6	8Ø31.8	331	9.5	400	457
2CLH18[4]	9	35	457	457	3.83	1	–	0.07	33.1	8Ø25.4	331	9.5	400	457
3SLH18[4]	10	35	457	457	3.87	1	635	0.09	25.6	8Ø31.8	331	9.5	400	457
2SLH18[4]	11	35	457	457	3.83	1	508	0.07	33.1	8Ø25.4	331	9.5	400	457
2CMH18[4]	12	35	457	457	3.83	1	–	0.28	25.5	8Ø25.4	331	9.5	400	457
3CMH18[4]	13	35	457	457	3.87	1	–	0.26	27.6	8Ø31.8	331	9.5	400	457
3CMD12[4]	14	35	457	457	3.87	2	–	0.26	27.6	8Ø31.8	331	9.5	400	305
3SMD12[4]	15	35	457	457	3.87	2	635	0.28	25.5	8Ø31.8	331	9.5	400	102
(A1)–MCFS[5]	16	35	200	200	4.0	1	–	0.10	36.5	8Ø12.7	444	5.0	417	120
(B1)–MCFS[5]	17	35	200	200	4.0	1	–	0.20	36.5	8Ø12.7	444	5.0	417	120
(C1)–MCFS[5]	18	35	200	200	4.0	1	–	0.10	36.5	8Ø12.7	444	5.0	417	120
(B1)–HCFS[5]	19	36	200	200	4.0	1	–	0.40	36.5	8Ø12.7	444	5.0	417	120
(C1)–HCFS[5]	20	35	200	200	4.0	1	–	0.20	36.5	8Ø12.7	444	5.0	417	120
FC4[6]	21	35	915	457	6.7	5	610	0.00	19.7	16Ø25.4	433	9.5	331	406
FC5[6]	22	35	915	457	6.7	6	610	0.00	20.6	16Ø25.4	433	9.5	331	406
FC15[6]	23	35	457	457	6.7	4	610	0.00	28.7	8Ø25.4	433	9.5	331	406

b, h: cross section width and height, respectively;L_s/d: aspect ratio; l_s: lap–splice length; *P*: axial load as % of $f_c{}'A_g$; $f_c{}'$: concrete strength; D_{bl},f_{yl}: diameter and yield stress of longitudinal Reinf.; d_t,f_{yh}: diameter and yield stress of stirrups; *s*: spacing of stirrups; angleθ: inclination of the compression stresses according to CBPapproach with respect to the longitudinal member's axis.[1]Woods and Matamoros (2010);[2] Lam et al (2003);[3]Sezen and Moehle (2004);[4]Lynn at al (1996);[5]Yavari et al (2009));[6]Aboutaha et al (1996 and 1999).

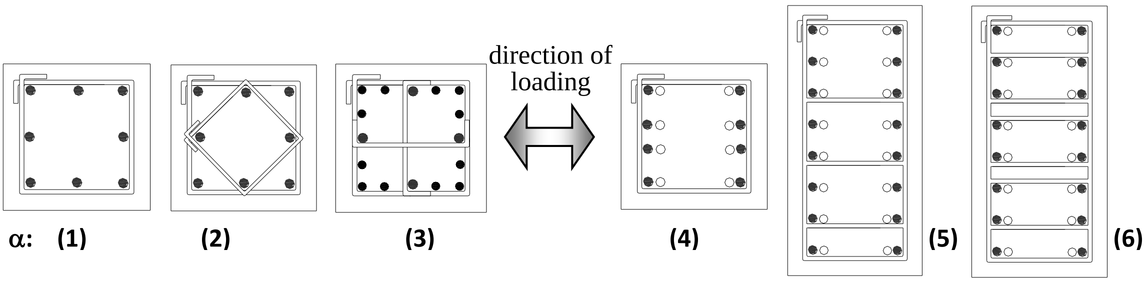

Figure 1. Cross section patterns of the specimens considered – in accordance with Tab. 1

3. DETERMINING THE COMPONENT OF UNCERTAINTY

To illustrate the uncertainty and scatter in the current state of the art regarding shear strength estimation for reinforced concrete members the first four of the specimens listed in Tab.1, which had failed in shear prior to yielding of the critical section are used as reference, as the experimental shear force sustained may be compared directly to the nominal calculated shear strength V_n before any degradation takes place. Analytical strength estimations are obtained from expressions included in the current assessment standards (i.e. the Model Code 2010, the EC8-III, and the ASCE/SEI 41). An enhanced version of the expression provided by ASCE/SEI 41 for the concrete contribution (Table 3),is that of the CBP which includes an enabling check that the cracks must have closed in order to account for this contribution (i.e., $N/A_g f_c^{'} > (\rho_{s1}-\rho_{s2}) \times f_y/f_c^{'}$) according with Pantazopoulou and Syntzirma (2010). Figure 2(a) plots results from various alternative estimations of prevailing columns strength for the four columns (i.e., the least lateral force estimate required to sustain either flexural failure or shear failure according with the various alternative assessment models mentioned). Note the scatter between the calculated alternatives and the test result. Figure 2(b) plots the estimated strength at shear failure against the test values. The test and calculated values of rotation capacity, θ_u, of the four specimens, is given in Fig. 2(c); these are obtained from the explicit expressions provided by the Assessment Standards. Here, in order to test the accuracy of the rotation expressions of the CBP (this method associates θ_u to the chord rotation at the onset of localization of failure in the weakest mechanism of resistance), shear strength V_n was set equal to the test value, V_{test} [Syntzirma and Pantazopoulou 2010]. The estimated chord rotation at loss of axial load capacity as estimated by ASCE/SEI 41 is also plotted in Fig. 2(c).

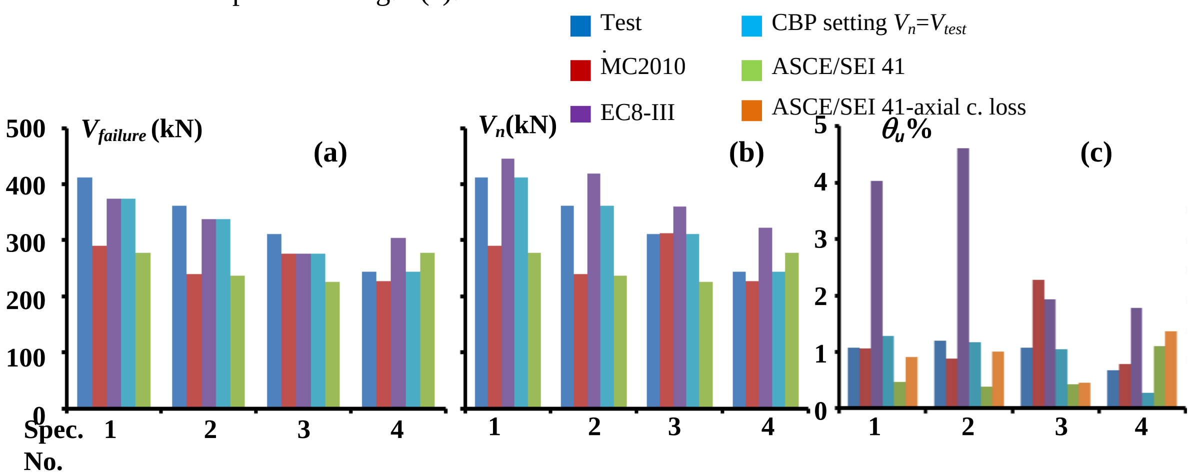

Figure 2. Comparison of (a) prevailing columns strength, (b) shear strength and (c) ultimate deformation (rotation capacity θ_u), between test values and Models estimations – in accordance with Tab.1

The scatter between the various alternatives illustrates the current state of understanding of seismic shear – note that the examples concerned elastic (prior to flexural yielding) reported modes of shear failure. It is also worth noting that the fundamental approach of the CBP model performed well with respect to the deformability estimates when the shear strength uncertainty was mitigated. This finding underscores the significance of correctly estimating shear strength as a crucial step towards reducing the reported scatter.

It was mentioned before that the inclination of the sliding plane (i.e. the angle between the principal diagonal tension crack that identifies shear failure and the member axis) controls both the so-called concrete contribution component, V_c, (through the inclination of the compressive strut parallel to the crack) and the number of stirrups mobilized in transverse tension; the latter has been traditionally associated with a 45^o Mörsch-type truss, which appears to disagree with experimental evidence. Figure 3 highlights the observed plane of failure and the number of stirrups mobilized in the case of the first four specimens listed in Table 1 (elastic shear failures). Considering the development capacity of the typical stirrup from the point of intersection with the diagonal tension crack to the hook end (the corresponding lengths are specified on Fig. 3), the estimated web steel contribution, V_w, as determined from the CBP model for the example columns are listed in Table 2. The difference between V_{test} and V_w is the estimated concrete contribution, V_c, which is given in the last row of the table. This is compared in Fig. 4 (a), with the analytical estimates obtained from a few well known models and Code expressions (listed in Table 3).

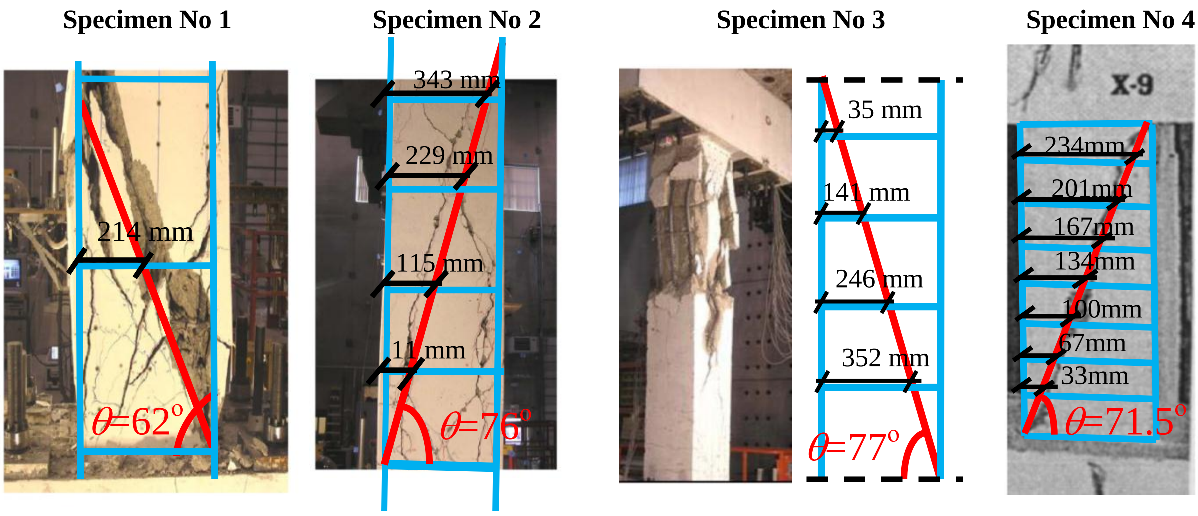

Figure 3. Test Specimens No 1 to 4. Formation of diagonal cracking.

Table 2. Calculation of the real concrete contribution in shear resistance with respect toFig. 3.

	Specimen No 1	**Specimen No 2**	**Specimen No 3**	**Specimen No 4**
V_{test}	412	361	311	244
V_w meas.(kN)	142	154	172	96
V_c calc. (kN)	270	207	139	148

Table 3. Expressions for the calculation of concrete contribution.

Model Code 2010	$V_{Rd,c}=k_v\sqrt{f_{ck}}zb_w$
EC8-III	$0.16\cdot\max(0.5;100\rho_{tot})\cdot\left(1+0.16\min\left(\frac{L_s}{h}\right)\cdot\sqrt{f_c}\cdot 0.8A_g\right)+\min\left(N;0.55A_c f_c\right)\quad (MPa)$
CBP model	if $\frac{N}{A_g\cdot f_c'}\ge(\rho_{s1}-\rho_{s2})\frac{f_y}{f_c'}\rightarrow V_c=k(\mu_\Delta)\cdot 0.5\sqrt{f_c'}\cdot\left(\frac{d}{L_s}\sqrt{1+\frac{N}{0.5\sqrt{f_c'}\cdot A_g}}\right)\cdot A_g;(MPa)$ otherwise $V_c=0$
CBP-modified	if $\frac{N}{A_g\cdot f_c'}\ge(\rho_{s1}-\rho_{s2})\frac{f_y}{f_c'}\rightarrow V_c=k(\mu_\Delta)\cdot 0.5\sqrt{f_c'}\cdot\left(\frac{d}{L_s}\sqrt{1+\frac{N}{0.5\sqrt{f_c'}\cdot A_g}}\right)\cdot c\cdot b_w;(MPa)$ otherwise $V_c=0$
Tureyen&Frosch 2003	$V_c=5\sqrt{f_c'}b_wc\quad(psi)$
ASCE/ SEI 41	$V_c=\left[\frac{0.5\sqrt{f_c}}{L_s/d}\sqrt{1+\frac{N}{0.5A_g\cdot\sqrt{f_c}}}\right]\cdot 0.8A_g\quad(MPa)$
ACI318-99, eq.(11-3)	$V_c=2\sqrt{f_c'}b_wd\quad(psi)$

A significant parameter controlling the relevance of the analytical estimates with the experimental results appears to be the area of concrete section contributing to V_c (Table 3): in most cases, the assumed effective shear area was equal or nearly equal to the area of the cross-section web: $A_g=b_w d$, or $0.8A_g$, or zb_w (where z the depth of the Mörsch truss). Tureyen and Frosch (2003) use the depth of compression zone, instead, leading to a much better approximation of the results, although the expression was calibrated for beams, thereby not accounting for the effect of the axial load. The CBP approach, modified accordingly also illustrates improved correlation with the test results.

Figure 4 (b) plots the observed values for the angle of inclination of the shear sliding plane relative to the transverse axis of the member for all the cases examined; note that the angle ranges between 62° and 76°, i.e. very far from the 45° assumption. Thus, the compressive strut which is through to be approximately parallel to the sliding plane is very steep for columns as compared to what is observed in beam tests (i.e. tests with low axial load which have formed the basis of calibration of the Mörsch truss).

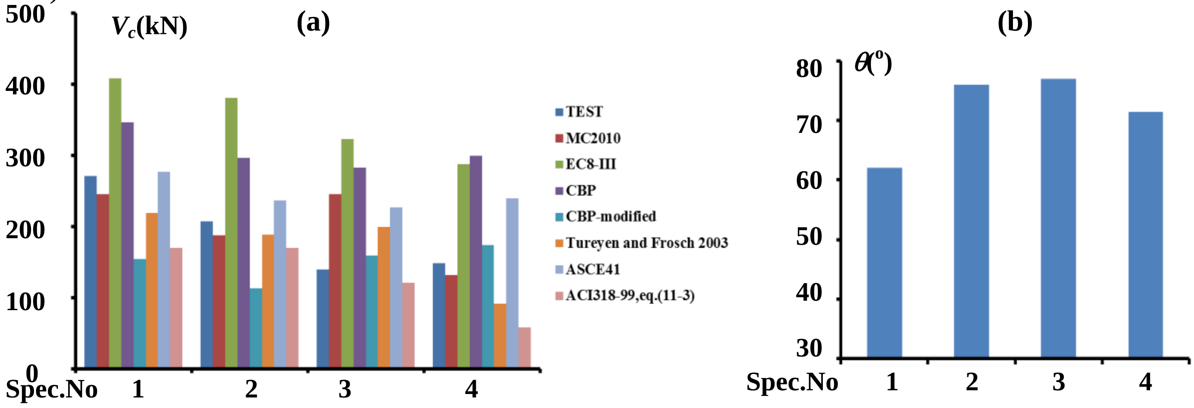

Figure 4. (a) Estimated concrete contribution to a member's shear strength (b) Observed angle θ of the principal sliding plane measured with respect to the column's transverse axis

4. SHEAR STRENGTH: NEW APPROACH AND CORRELATION WITH TESTS

In this section the concrete contribution component is established from first principles. As a point of departure it is clarified that concrete directly supports shear only over the compression zone of the member, c, where cracks may be assumed to have closed. So the effective area A_v, contributing to shear resistance is taken equal to $b_w \times c$. Here two different member cross sections of a column undergoing lateral sway under earthquake action are considered for analysis (Fig. 5). The cross section shown in Fig. 5(b) is located at the member end; forces F_c, C_{s2} and T_{s1} are the resultants of the compression stress block, stresses in compression reinforcement and tension reinforcement, respectively (ρ_{s1} and ρ_{s2} are the compression and tension reinforcement ratios, respectively, calculated over the area of the web, $b_w d$). Similarly, the cross section shown in Fig. 5(c) represents the nominal state of stress at the member's midpoint (section m).

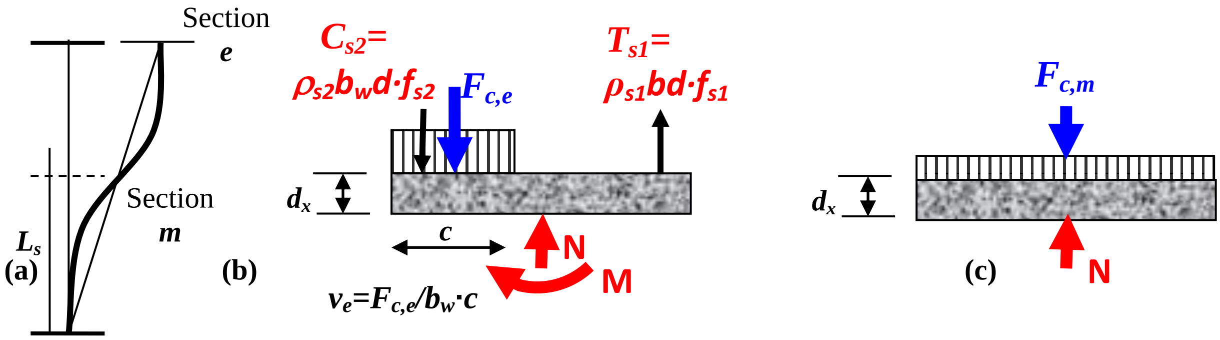

Figure 5. (a) Column under lateral sway, (b) Equilibrium of normal forces at section e, (c) Nominal normal forces at section m (actually the long. reinforcements might be in tension due to shear).

If ν is the mean axial stress of the column cross section in Fig.5 (b), the stress tensor in the compression zone is:

$$\underline{\sigma}=\begin{pmatrix}\nu & \tau\\ \tau & 0\end{pmatrix}\Rightarrow \sigma^{(e)}=\frac{\nu}{2}\pm\sqrt{\tau^2+\left(\frac{\nu}{2}\right)^2}\Rightarrow -f_{ctk}=\frac{\nu}{2}+\sqrt{\tau^2+\left(\frac{\nu}{2}\right)^2}\Rightarrow -\left(f_{ctk}+\frac{\nu}{2}\right)=$$
$$\sqrt{\tau^2+\left(\frac{\nu}{2}\right)^2}\Rightarrow \tau^2+\left(\frac{\nu}{2}\right)^2=\left(f_{ctk}+\frac{\nu}{2}\right)^2\Rightarrow \tau=\sqrt{f_{ctk}\cdot\left(f_{ctk}+\nu\right)}=f_{ctk}\cdot\sqrt{\left(1+\frac{\nu}{f_{ctk}}\right)} \tag{4.2}$$

where, at the onset of diagonal cracking of the web, the principle tensile stress $\sigma^{(e)}$ is limited by the tensile strength of concrete f_{ctk}=0.5$\sqrt{f_c}$, whereas $\nu=F_{c,e}/b_w c$ the mean normal concrete compressive stress in the end cross section (i.e. the compression force resultant at the end section normalized with the concrete area under compression). The shear stress τ is related to the flexural moment at the end cross section when considering that $V=M/L_s$ where L_s the member's shear-span:

$$\tau=\frac{V}{c\cdot b}=\frac{M}{c\cdot b\cdot L_s}$$

Upon substitution to (4.2), Eqn. 4.4 is obtained for ν:

$$\tau=\frac{M}{c\cdot b\cdot L_s}=f_{ctk}\sqrt{\left(1+\frac{\nu}{f_{ctk}}\right)}\Rightarrow \nu=\frac{\left(\frac{M}{x\cdot b\cdot L_s}\right)^2-f_{ctk}{}^2}{f_{ctk}{}^3} \tag{4.4}$$

The orientation of principal axes, θ, in the end cross section is obtained with reference to the longitudinal member axis, using basic mechanics according with Eqn. 4.5:

$$\tan 2\theta=2\cdot\tau/(\sigma_x-\sigma_y)=\frac{2f_{ctk}\cdot\sqrt{\left(1+\frac{\nu}{f_{ctk}}\right)}}{\nu}=2\frac{\sqrt{\left(1+\frac{\nu}{f_{ctk}}\right)}}{\nu/f_{ctk}};\;\; f_{ctk}=0.5\sqrt{f_c}\Rightarrow$$
$$\tan 2\theta=2\frac{\sqrt{\left(1+\frac{\nu}{0.5\sqrt{f_c}}\right)}}{\nu/0.5\sqrt{f_c}};\;\;\omega=\frac{\nu}{f_c}\Rightarrow \tan 2\theta=\frac{\sqrt{\left(1+2\omega\sqrt{f_c}\right)}}{\omega\sqrt{f_c}} \tag{4.5}$$

where ω represents the normalized stress ratio in the concrete compression zone of the member (note that the value of ω is much higher than $\nu_o=N/f_c{}'\cdot b_w\cdot d$ which represents the reported in tests, nominal axial load ratio, a value that occurs at the point of inflection in the absence of flexural moment).

Using the above equations, the only parameter to be defined is the stress level of the member at which shear cracking initiates in the compression zone. Defining this point in the resistance curve of the member, the values of acting moment $M_{sh,cr}$ and compression zone depth c can be easily calculated. Here it is implicitly assumed that the first main crack formation due to diagonal tension will also define the inclination of the shear sliding plane. As shown in Fig. 6 (a), extensive cracking generally precedes the onset of longitudinal reinforcement yielding as manifested by a substantial reduction of effective flexural stiffness, while the member is still in the apparent elastic range of response. A point of reference in defining the point of web cracking is that where the post cracking stiffness loss is severe so that the effective EI tends to its secant value at the onset of yielding (this corresponds to stabilization of cracking as identified by the red mark in Fig. 6 a and b).

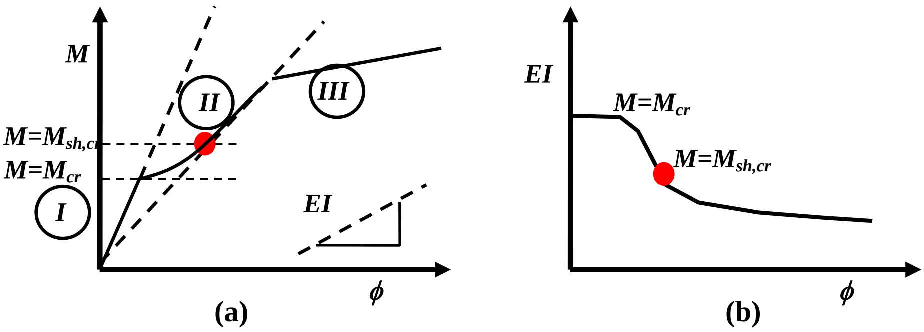

Figure 6. Defining the point of shear crack initiation

When applying Equation 4.5 to the specimens described in Table 1 it was found that the angle θ varies between 25^o to 35^o with respect to the member's longitudinal axis (this is a range of 65 to 55 degrees with respect to the transverse axis of the member, a finding that complies with the experimental values of Fig. 4 b). In this case the concrete contribution, is given by the shear stress resultant over the compression zone of the critical section, $V_c = \tau \cdot 0.8 b_w c$, whereas the corresponding steel contribution, V_s, is obtained from the sum of forces of the total number of stirrup legs parallel to the plane of action and intersected by the inclined crack plane:

$$\textbf{No of stirrups intersected by the shear plane:} \quad \frac{d-c}{s \cdot \tan\theta} \tag{4.6}$$

$$V_w = A_{s,tr} \cdot f_{y,tr} \cdot \frac{d-c}{s \cdot \tan\theta} \tag{4.7}$$

The methodology developed in this section was applied to the entire collection of tests studied in Table 1. Results are plotted for the nominal shear strength V_n in Fig. 7a whereas Fig. 7b plots the estimated specimen strength, $V_{failure}$, when considering the hierarchy of failure. Values in Fig. 7a with estimated shear strength higher than that measured in the tests do not necessarily imply lack of correlation: these are example where failure was eventually controlled by alternative modes as illustrated in Fig. 7b which compares the test value with the strength of the prevailing mode. Here, cases where the calculated values of $V_{failure}$ are equal although they are obtained from different models whereas the corresponding V_n values differ are again those that are controlled by an alternative, weaker mode of failure other than shear – e.g. flexural and lap-splice failure. Note the significant improvement in the estimated values when capacity-based prioritizing of failure is employed to organize the various mechanisms of resistance (CBP method, comparison of Fig. 7a with Fig. 7b) after the introduced modifications to the estimated plane of sliding and the effective area of the cross section contributing to shear resistance.

5. CONCLUSIONS

Through systematic evaluation of experimental results concerning brittle columns that failed in shear prior to flexural yielding under combined axial load and lateral load reversals, this paper explored the deficiencies in the existing methods of estimation of seismic shear strength of reinforced concrete members. Because shear strength is an essential tool in seismic assessment, used in order to: identify the strength hierarchy of the various mechanisms of resistance, to determine the prevailing mode of failure and eventually to estimate the dependable deformation capacity of reinforced concrete, it is essential for the improvement of performance based design that the excessive of scatter associated with the analytical methods of its estimation be mitigated. In this paper, an alternative method of calculation of both shear strength contributions (i.e. those owing to concrete and to web reinforcement) is established from first principles. An important outcome is the angle of inclination of diagonal tension failure in the critical zones of the member, which also defines the number of stirrups mobilized in tension to resist shear. It is concluded that, consistently with experimental evidence, the strut angle that accounts for seismic shear of columns is much steeper than the 45° assumption made in the established assessment standards. Test results are correlated successfully particularly when accounting for a reduced effective shear area (supporting the concrete contribution component) restricted to the core of the member's compression zone.

AKCNOWLEDGEMENT

Work presented in this paper was conducted under partial support from Institute for Construction Materials, University of Stuttgart, Germany and Demokritus University of Thrace, Greece.

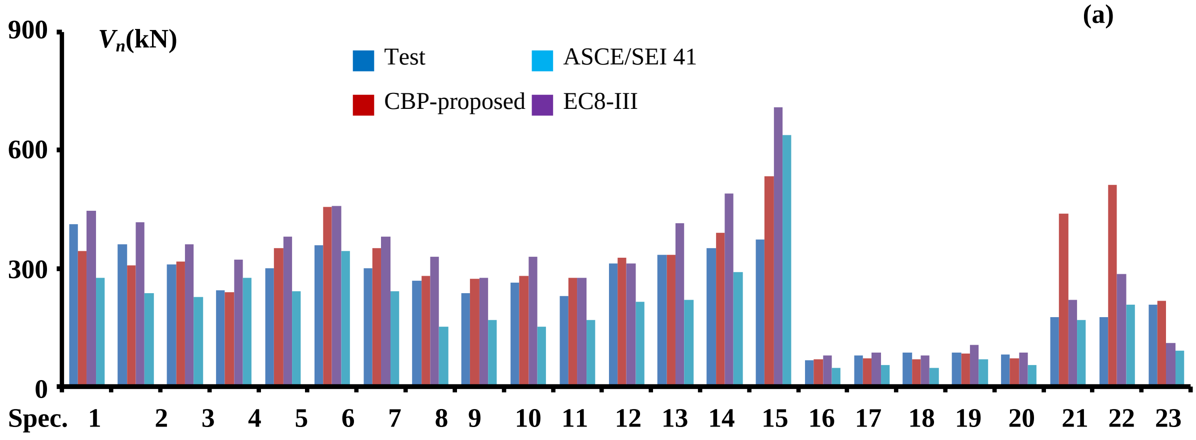

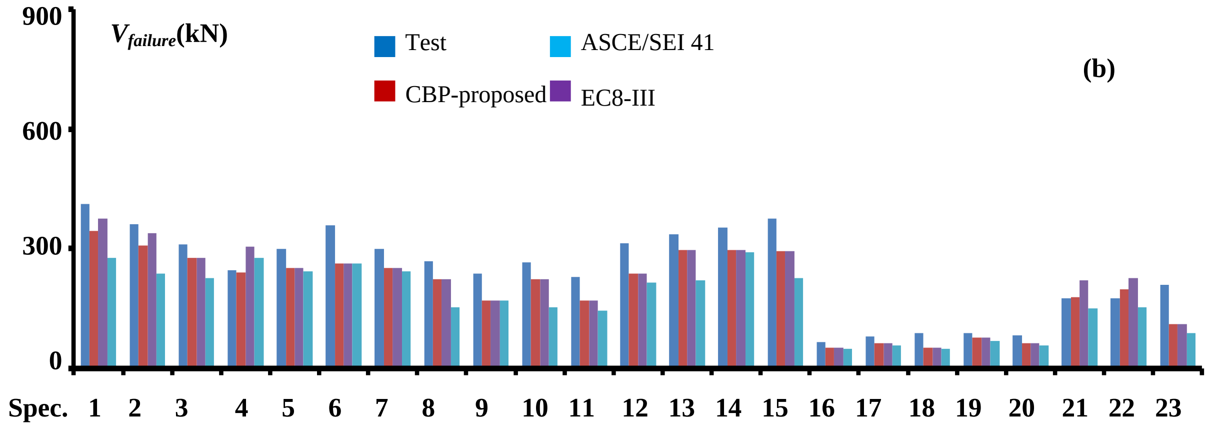

Figure 7. Comparative study of strength indices proposed by C.B.P. model, EC8−III, C.B.P. and ASCE/SEI 41 vs. the experimental values.

EXAMPLE

For the 1st specimen of the Table 1 (Woods and Matamoros 2010), here the shear strength V_n according to the new approach presented in chapter 4 is calculated.

$$f_{ctk} = \mathbf{0.5}\sqrt{f_c} = \mathbf{0.5}\sqrt{\mathbf{33}} = \mathbf{2.87}\ MPa$$

In order to form the diagram of how stiffness decays with increasing cross section curvature (Fig. 6b), fiber analysis for the end cross section till the point of yield is performed. The point where the first shear crack is formed and defines the moment $M_{sh,cr}$ is identified by the red mark on the Figure 8, and corresponds to a strain of 0.1‰ to the reinforcement under tension. In this case, $M_{sh,cr}$=197 kNm and the compression zone depth c is 337 mm.

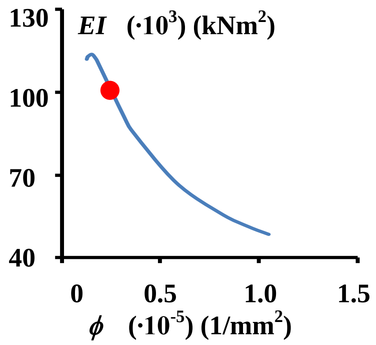

$$v=\left|\left(\left(\frac{197000000}{337\cdot457\cdot1472.5}\right)^2\Big/2.87^2\right)-1\right|\cdot 2.87=2.61MPa$$

$$\omega=2.61/33=0.08 \qquad \tan 2\theta=\frac{\sqrt{\left(1+2\cdot0.08\sqrt{33}\right)}}{0.08\sqrt{33}}=3.04\rightarrow\theta=35^o$$

No of stirrups crossed: 1. Therefore V_w=52 Kn

The shear stress over the compression zone is:

$$\tau=2.87\sqrt{\left(1+\frac{2.61}{2.87}\right)}=3.97MPa$$

Figure 8. Defining the point of shear crack initiation for the Spec. No. 1

And the concrete contribution to the member's shear capacity: V_c= $\tau\cdot0.8b_wc$=3.97·0.8·457·200=291 kN, where in this case the depth of the compression zone c is 200 mm, because corresponds to the cross section point of yield. The shear capacity of Spec.No.1 is: V_n=291+52=343 kN.

REFERENCES

Tureyen, A.K. and Frosch, R.J. (2003). Concrete shear strength: Another perspective. *ACI Structural Journal **10:5***,609-615.

Aboutaha, R.S., Engelhardt, M.D., Jirsa, J.O., and Kreger, M.E. (1996), Retrofit of concrete columns with inadequate lap splices by the use of rectangular steel jackets. *Earthquake Spectra* **12:4**,693-714.

Aboutaha, R.S., Engelhardt, M.D., Jirsa, J.O., and Kreger, M.E. (1999), Experimantal investigation od seismic repair of lap splice failures in damages concrete columns. *ACI Structural Journal **96:2***,297-306.

Lam, S.S.E., Wu, B., Wong, Y.L., Wang, Z.Y., Liu, Z.Q. and Li, C.S. (2003), Drift capacity of rectangular reinforced concrete columns with low lateral confinement and high-axial load. *ASCE Journal of Structural Engineering **129:6***,733-742.

Lynn, A., Moehle, J.P., Mahin, S., and Holmes, W. (1996), Seismic evaluation of existing R.C. building columns. *Earthquake Spectra **12:4***,715-739.

Sezen, H. and Moehle, J. (2004). Strength and deformation capacity of R.C. columns with limited ductility. *13thWorld Conference on Earthquake Engineering*. No 279.

Woods, C. and Matamoros, A.B. (2010). Effect of longitudinal reinforcement ratio on the failure mechanism of R/C columns most vulnerable to collapse. *9thU.S. National and 10th Canadian Conference on Earthquake Engineering*. No 1636.

Yavari, S. Elwood, K., Lin, S. H., Wu, C.L., Hwang S.,J., and Moehle J. (2009). Experimental study on dynamic behavior of multi-story reinforced concrete frames with non-seismic detailing. *ATC & SEI 2009 Conference on Improving the Seismic Performance of Existing Buildings and Other Structures*. p.p.489-499.

ASCE/SEI 41 (2007). Seismic Rehabilitation of Existing Buildings, American Society of Civil Engineers.

CEB-FIP Model Code (2010). Chapter 6:Interface Characteristics; Chapter 7:Design.

Elwood, K., Matamoros, A., Wallace, J., Lehman, D., Heintz, J., Mitchell, A., Moore, M., Valley, M., Lowes, L., Comartin,C., and Moehle, J. (2007), Update to ASCE/SEI 41 Concrete Provisions. *Earthquake Spectra* **23:3**,493-523.

Eurocode 8 (2005). Design of structures for earthquake resistance – Part.3: Assessment and retrofitting of buildings, European Committee for Standardisation.

FEMA 356 (2000). Prestandard and commentary for the seismic rehabilitation of buildings, Federal Emergency Management Agency.

Pantazopoulou, V. and Syntzirma, D. (2009). Code expressions for deformation capacity of lightly reinforced concrete members – a comparative study. *ACES Workshop:Advances in Performance-Based earthquake Engineering*.

Syntzirma, D.V., and Pantazopoulou, S.J. (2006), Deformation capacity of R.C. members with brittle details under cyclic loads. ACI Special Publication **Vol. 236:** 1-22.

ACI 318-99 (1999), Building Code Reguirements for Structural Concrete, American Concrete Institute.

Syntzirma, D.V., and Pantazopoulou, S.J. (2010), Deformation capacity of lightly reinforced concrete members – comparative evaluation. *ACES Workshop:Advances in Performance-Based earthquake Engineering*, Series Geotechnical, Geological, and Earthquake Engineering, Vol. 13, Springer.